Materials & Design 185 (2020) 108276

Contents lists available at ScienceDirect

Materials & Design

journal homepage: www.elsevier.com/locate/matdes

Abnormally high strength and low electrical resistivity of the deformed Cu/Mg-composite with a big number of Mg-filaments

A.Yu Volkov [a, *], B.D. Antonov [b], E.I. Patrakov [a], E.G. Volkova [a], D.A. Komkova [a], A.A. Kalonov [a], A.V. Glukhov [a, c]

[a] Mikheev Institute of Metal Physics, Ural Branch, Russian Academy of Sciences, 18 S. Kovalevskaya St, Ekaterinburg, 620108, Russia
[b] Institute of High-Temperature Electrochemistry, Ural Branch, Russian Academy of Sciences, 20 Akademicheskaya St, Ekaterinburg, 620041, Russia
[c] Ural Federal University Named after the First President of Russia B.N.Yeltsin, 19 Mira St, Ekaterinburg, 620002, Russia

HIGHLIGHTS

- The theoretical estimation accuracy of the Cu/Mg-composite strength is highly dependent on the constituents ratio.
- A supersaturated Cu-based solid solution is formed at the interfaces of the Cu/Mg-composites as a result of SPD.
- The Cu/Mg-composite with minimal volume fraction of magnesium has abnormally high strength and low electrical resistivity.

GRAPHICAL ABSTRACT

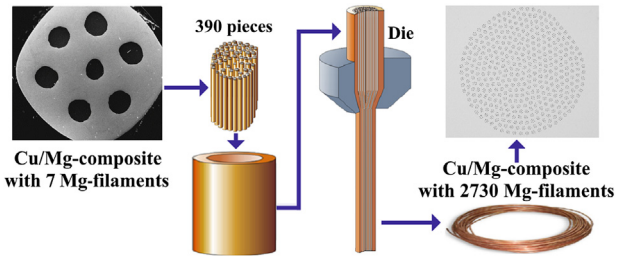

ARTICLE INFO

Article history:
Received 14 August 2019
Received in revised form
1 October 2019
Accepted 13 October 2019
Available online 18 October 2019

Keywords:
Bimetallic composite
Cu/Mg diffusion couple
Severe plastic deformation
Mechanical properties
Electrical conductivity

ABSTRACT

Cu/Mg-composites, the copper matrix of which contains 1, 7 and 2730 magnesium filaments, were obtained by hyrdoextrusion at room temperature. The structure, mechanical and electrical properties of the deformed composite rods and thin wires were investigated. The yield strength and electrical resistivity were theoretically calculated and these estimations were compared with the experimental results. The XRD-method allowed discovering a change of the lattice constant of the Cu-matrix under deformation of the composites. It has been concluded that, under severe plastic deformation, a supersaturated Cu-based solid solution forms on the Cu/Mg-interface. As a result, the strength of the deformed Cu/Mg-composite with minimal volume fraction but maximal surface area of magnesium is abnormally high. A thick Cu-sleeve provides low electrical resistivity of this Cu/Mg-composite. The obtained results can be used for the development of high-strength Cu-based conductors.

1. Introduction

Copper-based alloys with high strength and good electrical conductivity have shown great promise in many fields [1–3]. Severe plastic deformation (SPD) leading to ultrafine grained microstructure and nanoscale precipitation of the secondary phase is the most commonly used method for strengthening copper alloys. In recent times, there have been appearing more and more works investigating the structures and properties of conductive materials based on the Cu–Mg alloys strengthened by different SPD-methods [2–4]. Indeed, Mg is a cheap and non-toxic metal with low density. It is very important because, for example, conductive Cu–Be alloys have the highest strength but their disadvantages are toxicity and high cost [2]. According to Ref. [4], contact wires of the Cu–Mg alloys have great potential for commercial application, for example, to satisfy the needs of the high-speed electrical railways.

* Corresponding author.
E-mail address: volkov@imp.uran.ru (A.Yu Volkov).

https://doi.org/10.1016/j.matdes.2019.108276

In contrast to a large number of works concerning Cu–Mg-alloys, the studies of Cu/Mg-composites are not so numerous. One of a few examples is work [5], where Cu/Mg super-laminate composites were investigated in respect of their hydrogen absorption/desorption properties. Other properties of the composite samples were not studied in this work. Probably, the main reason that prevents the researchers from working on the creation of high-strength Cu/Mg-composites is related to doubts about the possibility of copper matrix reinforcement by introduction of noticeably less strong Mg-filaments into it.

Two kinds of intermetallic compounds (Cu_2Mg and $CuMg_2$) are observed in the Cu–Mg system (Fig. 1) [6]. Obviously, the eutectic reactions taking place on the interface will cause changes in physical and mechanical properties of the Cu/Mg-composites. In accordance with [7,8], the obtaining of multi-layered sandwiches based on Ti/Al or Mg/Al/Mg with intermetallic layers between metals was characterized by a significant improvement of mechanical properties. Moreover, it is known that even the immiscible elements may form supersaturated solid solution as a result of SPD-processing [9]. It may also be promising because the dissolution of Mg in the Cu-matrix leads to solid solution hardening, which increases the strength of Cu–Mg alloys up to a high level [2,3]. However, the solid solution formation on the interface of the Cu/Mg-composites during SPD has not been described yet.

The purposes of this study were (1) to develop a technique for fabrication of Cu/Mg-composites with various numbers and diameters of Mg-filaments, (2) to clarify the Mg-filament formation and evolution of the Cu/Mg-interface during the deformation process, and (3) to reveal the effect of the deformation on the microstructure, electrical and mechanical properties of these composites.

2. Materials and methods

In this study, there were obtained and investigated composite rods and wires, which contained 1, 7 and 2730 Mg-filaments inside the Cu-matrix. Further, we will indicate the numbers of magnesium filaments in the designations of composites. For example, a composite containing 2730 Mg-filaments will be noted as follows: Cu/2730 Mg-composite.

Fig. 2 illustrates the method applied to fabricate Cu/Mg-composites in the present work. At the first step, we placed a magnesium workpiece of 12 mm in diameter in a Cu-container of 18 mm in diameter (see the left part of Fig. 2a). To obtain Cu/1 Mg-composite, this "assembly" was hydrostatically extruded at room

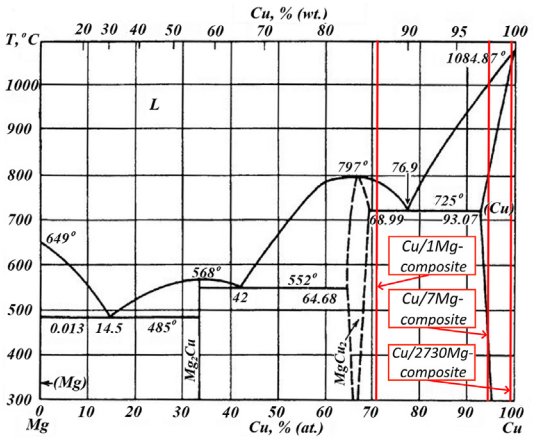

Fig. 1. Phase diagram of the Cu–Mg system [6]. Red lines mean the Cu/Mg-ratio in the composites under investigation.

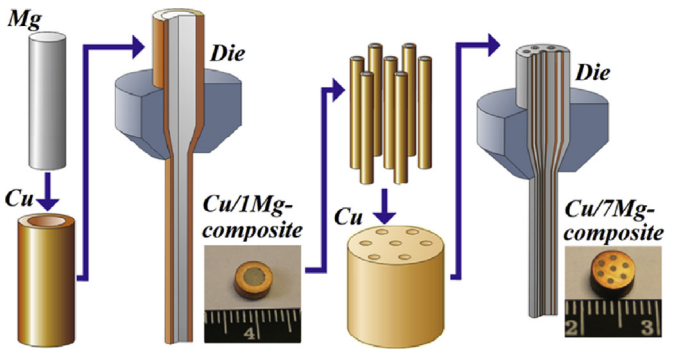

Fig. 2. Schematic diagram showing the process of making composite rods with 1 and 7 Mg-filaments in the Cu-matrix.

temperature through a die of 10 mm in diameter. Then, the hydroextrusion process was consecutively repeated using dies of Ø6 mm and Ø3 mm. To fabricate a Cu/7 Mg-composite rod, the Cu-container of 21.5 mm in diameter with 7 holes of Ø3 mm was used (see the right part of Fig. 2). One hole was located at the center and other six ones were located about 5.5 mm away from the center and 60° away from each other. 7 rods of the Cu/1 Mg-composite of 3 mm in diameter were tightly inserted into these holes. Then, this copper-magnesium assembly was consecutively submitted to hydroextrusion through dies of Ø10 mm, Ø6 mm and Ø3 mm.

The Cu/2730 Mg-composite was made by the known method of accumulative drawing and bundling (ADB) [10]. For this purpose, an extruded 3-mm rod of Cu/7 Mg-composite was drawn to obtain wire of 0.5 mm in diameter. Then, 390 pieces of this thin composite wire were inserted into the Cu container, it was followed by room-temperature hydroextrusion repeated three times to obtain a rod of Ø3 mm (Fig. 3). Finally, the extruded 3-mm rods of Cu/1 Mg, Cu/7 Mg and Cu/2730 Mg-composites were drawn into wires with various diameters at room temperature.

Before the hydroextrusion, all Cu-containers, Mg-workpiece and Cu/Mg-composite wires were preliminary annealed at 200°C during 3 h. As we showed earlier [11], this thermal treatment leads to recrystallization of copper. Low-temperature treatment at 150–200°C causes some increase in strength and plasticity of pre-deformed magnesium [12]. Moreover, as it was revealed in Ref. [13], the intermetallic compounds $CuMg_2$ and Cu_2Mg can grow in Cu/Mg diffusion couple only at temperatures above 200 °C. Therefore, we came to the conclusion that annealing at 200°C would not lead to the formation of new phases at the Cu/Mg interface.

The volume fractions of Cu and Mg in each of the studied composites are listed in Table 1. To obtain these results, we took the sizes of the Cu-containers and Mg-filaments before the hydroextrusion. Based on the volume fractions of copper and magnesium,

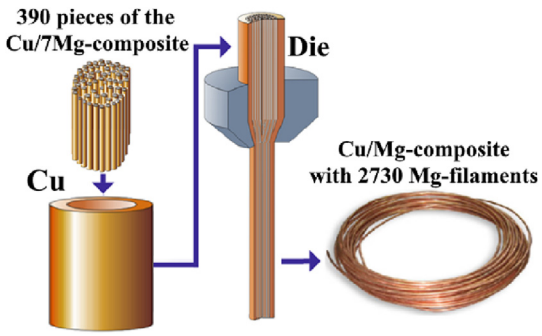

Fig. 3. Schematic diagram showing the process of making a composite rod with 2730 Mg-filaments in the Cu-matrix.

their contents in weight and atomic percent were calculated in each of the studied composites (Table 1).

The Cu/Mg-ratio in the composites can be compared with the phase diagram (see the red lines in Fig. 1). The composition of the Cu/1 Mg-composite is on the left of the eutectic composition (76.9 at.%Cu - 23.1 at.%Mg) due to a surplus of magnesium. The Cu/7 Mg-composite contains much less magnesium and this composition is in the region of the fcc-Cu(Mg) solid solution at high temperatures, but the two-phase structure (fcc-Cu(Mg) + Cu_2Mg) forms in it during the cooling. The content of magnesium in the Cu/2730 Mg-composite is very low. The single-phase fcc-Cu(Mg) solid solution (Fig. 1) is formed in the alloy of such a composition.

The electrical resistivity of the samples 0.25 mm in diameter was measured by the four-probe technique at direct current of 20 mA. The absolute deviation of the electrical resistivity measurements was found to be $\Delta\rho = \pm\ 0.04 \times 10^{-8}\ \Omega\,m$. The strength properties of the composite wire of 1.5 mm in diameter and 30 mm long were checked by tensile testing using an Instron 5982 test machine with the strain rate equal to 3 mm/min. QUANTA 200 FEI and INSPECT F scanning electronic microscopes (SEM) were used to characterize microstructure of the composites. The X-ray diffraction (XRD) analysis was performed using a Rigaku DMAX 2200 diffractometer by the method of continuous recording at a speed of 4°. CuKα radiation was monochromatized with a graphite single crystal.

In the course of our investigation, we worked with samples having different deformation strains. As a rule, the true strain (e) is defined by equation [14]:

$$e = \ln (S_o/S_f), \quad (1)$$

where S_o and S_f are the initial and final cross section areas of the sample, respectively. However, in our case, formula (1) may be used to evaluate the true strain of the Cu/1 Mg-composite samples only. Indeed, we repeated the deformation processing cycle a few times and the diameter of the sample increased when we moved from the Cu/1 Mg-composite to the Cu/7 Mg-composite (and also when we moved from the Cu/7 Mg-composite to the Cu/2730 Mg-composite). Obviously, in our case, S_o and S_f in eq (1) are the initial and final cross section areas of the Mg-filament that makes it difficult to use this formula.

For easy estimating the accumulated deformation strain (η) in our composites, we upgraded formula (1). The details of this procedure can be found in Appendix A.

3. Results

3.1. Microstructures of the composites

Fig. 4 shows two Cu/1 Mg-composite samples. In the right part of the Fig. 4, there is an extruded rod with 3 mm diameter. In the left part of Fig. 4, there is a thin wire of Ø0.25 mm obtained by drawing of the rod. In order to show the shining magnesium core, the copper matrix was intentionally removed from the tip of this wire.

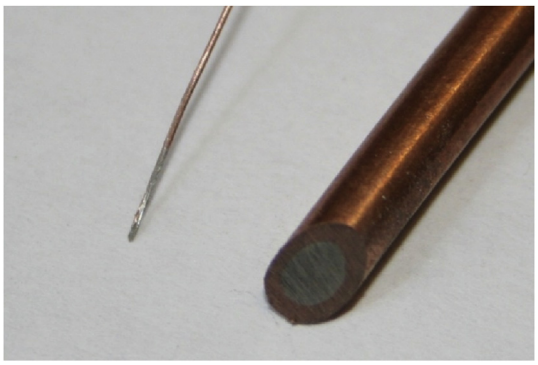

Fig. 4. Views of the Cu/1 Mg-composite makes: on the right-hand side – the rod of 3 mm in diameter after hydroextrusion; on the left-hand side – the wire of 0.25 mm in diameter, which was made from the rod by drawing.

The typical microstructures of the as-extruded rods of the Cu/7 Mg-composite and Cu/2730 Mg-composite are illustrated in Fig. 5 and Fig. 6, respectively. It is clearly seen that the cross section of the Mg-filaments is changing from round in the Cu/7 Mg-composite to oval in the Cu/2730 Mg-composite. This is due to a change in the material forming mechanisms with a change in the deformation process.

The Cu/7 Mg-composite rod in Fig. 5 was obtained by hydroextrusion, i.e. the deformation of the Mg-filaments inside the Cu-matrix took place practically under the conditions of all-round compression. In this case, the Mg-filaments kept their cylindrical shape. In turn, to obtain the Cu/2730 Mg-composite in Fig. 6a the extruded Cu/7 Mg-composite rod was drawn up to thin wire of 0.5 mm in diameter (Fig. 6b). The deformation by drawing goes together with a strong tangential flow of the outer layers of the material. It causes a change in the shape of the outer 6 Mg-filaments in the Cu/7 Mg-composite from round to curved ellipse.

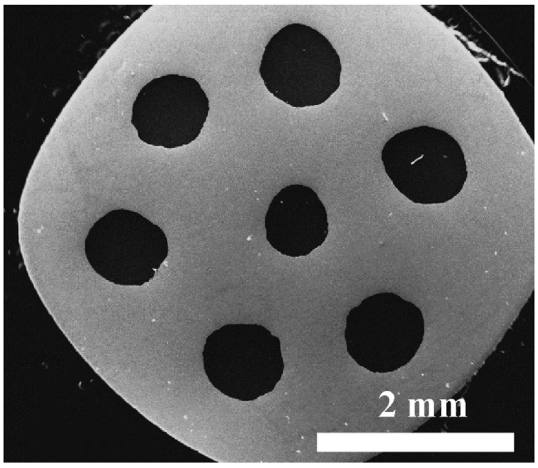

Fig. 5. Structure of the as-extruded Cu/7 Mg-composite rod of 6 mm in diameter.

Table 1
The Cu/Mg-ratio in the obtained composites.

Composite	Number of the Mg-filaments	Content of the constituent metals					
		Volume fraction, %		Wt. %		At. %	
		Cu	Mg	Cu	Mg	Cu	Mg
Cu/1 Mg	1	55.5	44.5	86.4	13.6	70.9	29.1
Cu/7 Mg	7	91.4	8.6	98.2	1.8	95.3	4.7
Cu/2730 Mg	2730	97.9	2.1	99.6	0.4	98.9	1.1

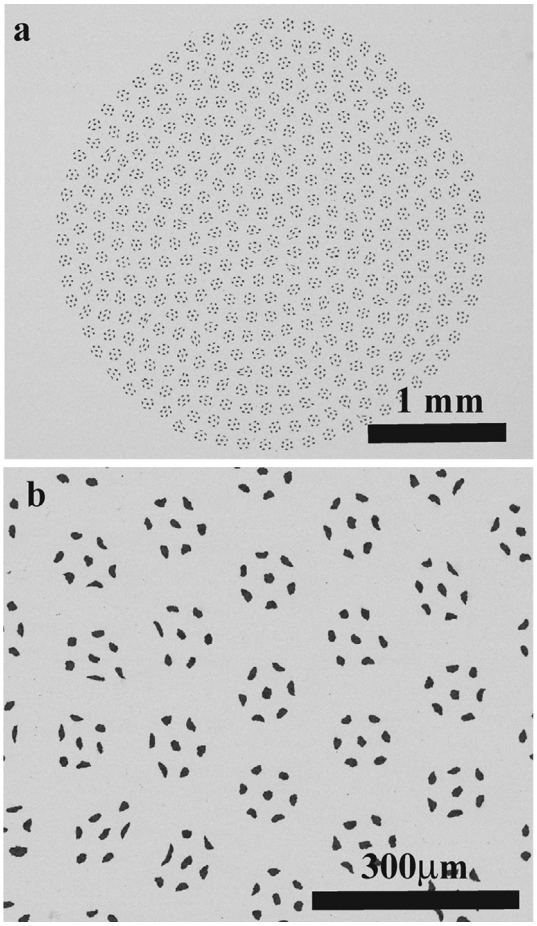

Fig. 6. Structure of the as-extruded Cu/2730 Mg-composite rod of 6 mm in diameter: (a) cross section view and (b) zoom of the central area of the microstructure shown in (a).

However, the Mg-filament, which is located in the center of the Cu/7 Mg-composite, is under all-round compression conditions even at drawing. Almost all these Mg-filaments remain round in the Cu/2730 Mg-composite (Fig. 6b).

It is clearly seen in Figss. 4–6 that, when the number of the Mg-filaments rises, the volume fraction of Mg dramatically drops. Above, we obtained the same result based on calculations (see Table 1). It is known that the ratio of components does not play a critical role in the formation of composite materials. As it was shown in Ref. [15], the structure and properties of composites greatly depend on the nature of the constituent metals and individual layer thicknesses. Therefore, it is necessary to take into account the diameter of Mg-filaments and the area of all interfaces.

For each of the investigated composites the interface surface area per unit volume was calculated (Table 2). It was determined as the ratio of the sum of the perimeters of all Mg-filaments to the cross-sectional area of the composite sample.

The calculations were performed for composite samples with 3 different cross sections: the workpiece before hydroextrusion, the wire with 1.5 mm diameter (they are samples for the mechanical test) and the thin wire with 0.25 mm diameter (they are samples for the resistometric study). The calculations performed show that the area of Cu/Mg interfaces grows with the increase in number of the magnesium filaments. It should be recalled that in the composites under investigation, when the number of the Mg-filaments increases, the volume fraction of magnesium decreases dramatically (Table 1). Thus, the Cu/2730 Mg-composite with the minimal magnesium content has the highest interface surface area per unit volume. The interface surface area is also affected by the change in diameter of the composite. As shown in Table 2, the interface surface area per unit volume of the composite increases almost two orders of magnitude when the sample diameter decreases to 0.25 mm.

Table 3
Densities of the Cu/Mg-composites.

	Density, g/cm^3	
	Experiment	Calculation
Cu/1 Mg-composite	5.5	5.7
Cu/7 Mg-composite	7.6	7.5
Cu/2730 Mg-composite	8.7	8.6

3.2. Densities of the composites under investigations

The density values of Cu/Mg-composites were determined experimentally using the bars with a diameter of 6 mm. The density of the Cu/1 Mg-composite is equal to 5.5 g/cm^3. It is significantly lower than that of the pure copper. Higher copper content in the Cu/7 Mg-composite leads to an increase in its density up to 7.6 g/cm^3. The density of the composite containing 2730 Mg-filaments (~ 8.7 g/cm^3) has a little difference compared to that of the pure copper. All the obtained results are summarized in Table 3.

However, the densities of the investigated composites are easy to calculate using the volume fractions of the components from Table 1. The results of these calculations are also listed in Table 3. It has been found that there is some difference between the experimental density and the calculation results. The simplest explanation of such divergences may be as follows. For our calculation, we took the sizes of the Cu-container and Mg-(or Cu/Mg-) wires before hydroextrusion. However, during the deformation of the Cu/Mg-composites, the copper is flowing somewhat faster than the magnesium. As a results, after hydroextrusion, the tailpiece of the composite rod consists of the Cu-sleeve only without the Mg-core inside it. We cut off this part as a waste. Based on these arguments, it is possible to conclude that the volume fractions of copper and magnesium listed in Table 1 are accurately determined for the non-deformed workpieces only. The Cu/Mg-ratio will change a little when making the composite rods and wires. As a result, the densities of the same Cu/Mg-composites of different diameters will

Table 2
Diameters of Mg-filaments and volume fractions of the Cu/Mg-interface in different samples of the studied composites.

Composite	Workpiece (before hydroextrusion)		Wire Ø1.5 mm (for the tensile tests)		Wire Ø0.25 mm (for the resistometric study)	
	Mg-filament diameter, mm	Volume fraction of the Cu/Mg-interface, mm^{-1}	Mg-filament diameter, mm	Volume fraction of the Cu/Mg-interface, mm^{-1}	Mg-filament diameter, μm	Volume fraction of the Cu/Mg-interface, mm^{-1}
Cu/1 Mg	12	0.15	1.0	1.78	170	10.87
Cu/7 Mg	2	0.12	0.14	1.74	23	10.32
Cu/2730 Mg	0.047	1.13	0.003	14.85	0.5	97.71

also be somewhat different. As a whole, the discrepancy between listed in Table 1 and true values of the Cu/Mg-ratio in the composites is small and can't bring any mistakes in our results below.

3.3. Mechanical properties of the Cu/Mg-composites

At present, there is established a clear relationship between the mechanical properties of a composite and its constituents [1,7,16]. For example, in work [17], the rule of mixtures (ROM) was used, to calculate the strength of bimetal composites based on Al and Mg alloys. However, this approach has some limits. It was shown in Ref. [17] that the ROM works well only if the layer thickness or the filament diameter lays within the millimeter scale. Besides that, no new phase should be formed at the interface during the process of composite obtaining.

We decided to check the applicability of the ROM calculation for the yield strength estimation of the deformed Cu/Mg-composites in our work. It is very interesting, because the diameter of the Mg-filaments changes significantly in the composites under investigation (see Figss. 4–6). In addition, we believed that the intermetallic compounds are not formed at the Cu/Mg interface during the fabrication of our composites.

Taking into account the views presented in Refs. [7,17], the yield strength of the bimetal composite (σ_{com}) can be calculated by the following equation:

$$\sigma_{com} = \sigma_{Cu} \times V_{Cu} + \sigma_{Mg} \times V_{Mg} \quad (2)$$

where, σ_{Cu} (σ_{Mg}) and V_{Cu} (V_{Mg}) are the yield strength and volume fraction of the Cu/Mg-composite constituents (note, that $V_{Cu} + V_{Mg} = 1$). As it was convincingly demonstrated in Ref. [17], the way to measure the mechanical properties of each constituent affects the deviation of the ROM predictions from the experimental results. Therefore, it is very important to measure the strength of the Cu- and Mg-samples directly cut from the composite but not from monolithic products.

In order to obtain the accurate strength of deformed magnesium for the ROM calculations, we took the extruded Cu/1 Mg-composite rod, cut it lengthwise and pulled the Mg-core out of it. The copper samples for testing were obtained by hydroextrusion according to the scheme used in the preparation of the Cu/1 Mg-composite (Fig. 2). The calculated values of the yield strengths of the Cu/Mg-composites and the results of their mechanical tests are shown in Table 4.

In accordance with formula (2), the yield strength of the Cu/1 Mg-composite was estimated as $\sigma_{0.2} \approx 237$ MPa. As shown in Table 4, the mechanical tests of the Cu/1 Mg-composite samples led to a different result $\sigma_{0.2} = 290$ MPa. We believe that the experimental result is largely deviate from the ROM calculation due to the fact that the strain hardening behavior of Mg (with the hexagonal close-packed crystal lattice) is quite different from Cu (with the face centered crystal lattice). The same conclusion was made earlier by the authors of [17]: the experimental flow curve of the bimetal composite rod, fabricated from two Al-alloys, had good agreement with the prediction, while that of the Al/Mg-composite showed a great deviation from the calculated one.

The experimental and theoretical yield strengths of the Cu/7 Mg-composite were close (322 and 328 MPa, respectively). Probably, in this case, the mechanical properties of the samples are mainly determined by the copper matrix and the contribution of magnesium is insignificant due to the smallness of its volume. However, this assumption does not work when considering the Cu/2730 Mg-composite. Based on the ROM calculations, the yield strength of this composite should be slightly lower than that of copper. However, the yield strength of the Cu/2730 Mg-composite is 381 MPa and this value significantly exceeds the yield strength of the extruded copper (350 MPa). It may be concluded that the experimental strength of the Cu/2730 Mg-composite is abnormally high. The elucidation of this phenomenon nature is of undoubted scientific interest. As for practical application, only a good combination of high strength and low electrical resistivity will make the Cu/Mg-composites interesting for that.

Table 4
Electrical resistivity and yield strength of the deformed Cu, Mg and Cu/Mg-composites.

	Specific electrical resistivity, ρ, 10^{-8} Ω m		Yield strength, $\sigma_{0.2}$, MPa	
	Experiment	Calculation	Experiment	Calculation
Copper (Cu)	1.83	–	350	–
Magnesium (Mg)	4.85	–	97	–
Cu/1 Mg-composite	2.35	2.53	290	237
Cu/7 Mg-composite	2.07	1.93	322	328
Cu/2730 Mg-composite	1.84	1.85	381	346

3.4. Electrical properties of the Cu/Mg-composites

Work [15] gives a detailed review of the models, which have been proposed before to describe the relationship between the resistivity and the individual features of different composites. Based on these results, in our work the electrical resistivity of the as-extruded Cu/Mg-composites (ρ_{com}) were estimated according to the known formula for the parallel conductors. It should be noted that the electrical resistivity of numerous metallic composites is determined by the defect scattering, phonon scattering, impurity scattering, interface scattering, and grain boundary scattering [15]. It is important to take into account all above contributions to the electrical resistivity of a composite when the thickness of the constituent metal layers decreases to the nanolevel. As it is clearly seen in Figs. 4–6 and Table 2, the diameters of the Mg-filaments in our composites are very far from nanosize. Therefore, we ignored the influence of any factors of scattering in determining of the electrical resistivity.

The electrical conductivity of the Cu/Mg-composites was determined by summing up the electrical conductivity of each component of the composite taking into account its volume fraction according to the formula:

$$1/\rho_{com} = V_{Cu}/\rho_{Cu} + V_{Mg}/\rho_{Mg} \quad (3)$$

where V_{Cu} and V_{Mg} are volume fractions of copper and magnesium in the composite (see Table 1), ρ_{Cu} and ρ_{Mg} are specific electrical resistivity of copper and magnesium.

By simple transformations of eq (3), we obtain the formula for calculating the electrical resistivity of the Cu/Mg-composites:

$$\rho_{com} = \rho_{Cu} \times \rho_{Mg} / (V_{Cu} \times \rho_{Mg} + V_{Mg} \times \rho_{Cu}) \quad (4)$$

Obviously, accurate calculations of the as-extruded Cu/Mg-composites resistivity require using the resistivity values of the SPD-samples of copper and magnesium. After the hydroextrusion and drawing with accumulated strain $\eta \approx 6.0$, the specific electrical resistivity of the copper is: $\rho_{Cu} = 1.83 \times 10^{-8}$ Ωm. The electrical resistivity of the Mg-core cut from the deformed Cu/1 Mg-composite rod is: $\rho_{Mg} = 4.85 \times 10^{-8}$ Ωm.

The results of the calculations are presented in Table 4. The calculated value of the specific electrical resistivity of the deformed Cu/1 Mg-composite is: $\rho_{Cu/1Mg} \approx 2.48 \times 10^{-8}$ Ωm. It regularly drops to $\rho_{Cu/7Mg} \approx 1.93 \times 10^{-8}$ Ωm in the Cu/7 Mg-composite due to an increased content of copper. The content of copper in the Cu/2730 Mg-composite is the highest. As a result, its specific electrical

resistivity ($\rho_{Cu/2730Mg} \approx 1.85 \times 10^{-8}$ Ωm) is estimated as the lowest of all the investigated samples.

The theoretical estimates of the electrical resistivity were experimentally verified by the resistometric study of the deformed Cu/Mg-composite wires of 0.25 mm in diameter (Table 4). In general, it could be concluded that the method we used allows us to estimate the electrical resistivity of the Cu/Mg-composite conductors with an acceptable accuracy. It is clearly seen that the accuracy of our calculations increases with the amount of copper. Indeed, the electrical resistivities of the deformed Cu/1 Mg-composite and Cu/7 Mg-composite samples are somewhat different from the calculated values. The experimental value of the resistivity of the Cu/2730 Mg-composite is practically equal to the calculated one.

3.5. Temperature dependences of electrical resistivity

It is well known that the heat treatment induces changes in the microstructures of the constituent metals of the composites and leads to arising of new phases at their interface [18]. All these processes affect the physical and mechanical properties of the composites. Therefore, the temperature dependences of electrical resistivity upon heating and cooling at constant rates make it possible to visualize any structural or phase transformation taking place in the sample [19]. Moreover, a change in electrical resistivity in response to the heat treatment is important to judge about the thermal stability of the microstructure and properties of the composites.

Fig. 7 and Fig. 8 show the temperature dependences of the electrical resistivity obtained at heating (curves 1) and cooling (curves 2) of the deformed Cu/7 Mg-composite and Cu/2730 Mg-composite, respectively. These figures also show the temperature derivatives of the electrical resistivity versus the temperature, $d\rho/dT$ (curves 3), which are plotted only for the stage of heating (i.e. they correspond to curves 1).

Three stages of the rapid resistivity growth at heating of the Cu/7 Mg-composite are clearly visible in curve 1 in Fig. 7. Obviously, each of these stages is a response to any transformation in the sample. In the $d\rho/dT$ plot (curve 3), three narrow peaks correspond to these stages. The peak intensity at 730°C is so great that its top was cut off. These peaks at ~490°C, ~560°C and ~730°C fully match the temperatures of the eutectic transformations in the phase diagram (Fig. 1). The eutectic transformations and formation mechanisms of microstructures on the Cu/Mg diffusion couple in a wide temperature range were well-investigated earlier. At heating above 400°C, two intermetallic compounds, Cu_2Mg and $CuMg_2$, are formed in the Cu/Mg diffusion layer [6,20]. At 485°C, the first eutectic reaction takes place at the phase boundary of the $CuMg_2$ intermetallic compound and Mg [13,21]. At further heating to 552°C, the next eutectic reaction takes place at the $Cu_2Mg/CuMg_2$ phase boundary [6,13]. The eutectic reaction at 725°C takes place at the boundary of the Cu_2Mg intermetallic compound and Cu-matrix [2]. Therefore, the temperature dependence of the electrical resistivity in Fig. 7 gives the complete idea of the processes that occur at different temperatures at the Cu/Mg interfaces.

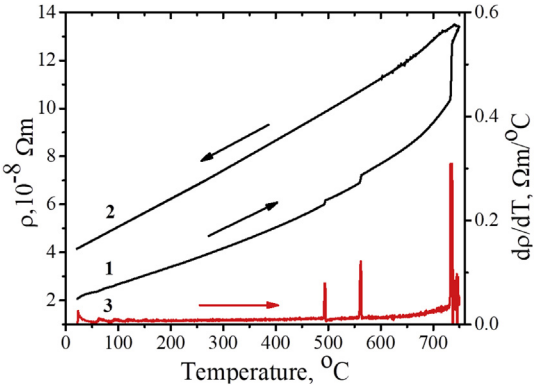

Fig. 7. Resistometric study results of the deformed Cu/7 Mg-composite: temperature dependences of the electrical resistivity obtained during the heating (curve 1) and cooling (2) and the temperature derivative (3), which corresponds to curve 1. The heating and cooling rate is 120°/hour.

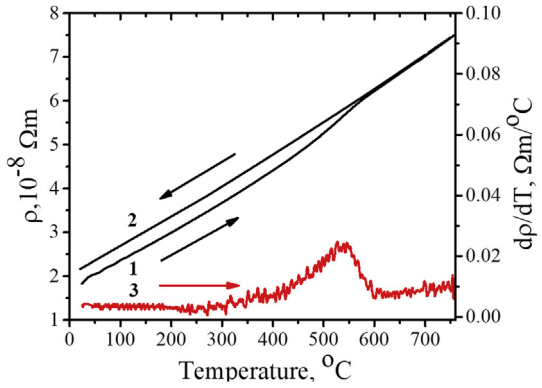

Fig. 8. Resistometric study results of the deformed Cu/2730 Mg-composite: temperature dependences of the electrical resistivity obtained during the heating (curve 1) and cooling (2) and the temperature derivative (3), which corresponds to curve 1. The heating and cooling rate is 120°/hour.

The resistometric study of the Cu/7 Mg-composite (Fig. 7) does not reveal any features at the melting point of magnesium (~650 °C). It allows us to conclude that, during the heating to this temperature, all magnesium atoms took part in diffusion reactions to form Cu_2Mg and $CuMg_2$ intermetallic compounds. In Fig. 7, it should be noted that structural transformations realized at heating of the Cu/7 Mg-composite lead to a strong increase in its electrical resistivity. Moreover, small increment of electrical resistivity is also seen at the cooling stage from 750 to 730 °C (curve 2 in Fig. 7). This may be due to the ongoing dissolution of the Cu-matrix in the molten eutectic. When cooled below the eutectic decomposition temperature, the temperature dependence of the electrical resistivity becomes linear. Therefore, there is no transformation in the Cu/7 Mg-composite at this stage. After cooling to room temperature, the electrical resistivity of the initially deformed Cu/7 Mg-composite increases almost two times (compare the position of the starting point of curve 1 with the position of the final point of curve 2). It can be assumed that during this experiment a significant amount of intermetallic phases with low electrical conductivity was formed in the Cu/7 Mg-composite.

Fig. 8 shows the results of the resistometric study obtained at heating and cooling of the Cu/2730 Mg-composite. These plots are significantly different from that of the Cu/7 Mg-composite (Fig. 7). Indeed, the temperature dependence of the resistivity obtained during heating (curve 1 in Fig. 8) does not have sharp visual changes. Moreover, when heated to 450 °C, the dependence is almost linear. With further heating, electrical resistivity grows some faster. A very wide peak on the $d\rho/dT$ plot corresponds to this region, the peak maximum being at ~530°C (curve 3 in Fig. 8). During the cooling of the Cu/2730 Mg-composite, the plot of the temperature dependence of the resistivity has the linear form (curve 2 in Fig. 8). Also, a very slight difference is in the resistivity values of the Cu/2730 Mg-composite before and after the experiment with heating of the sample to 750° followed by cooling (Fig. 8).

3.6. X-ray analysis

The X-ray diffraction patterns of the Cu/Mg-composites are shown in Fig. 9a. These spectra were obtained from the centers of

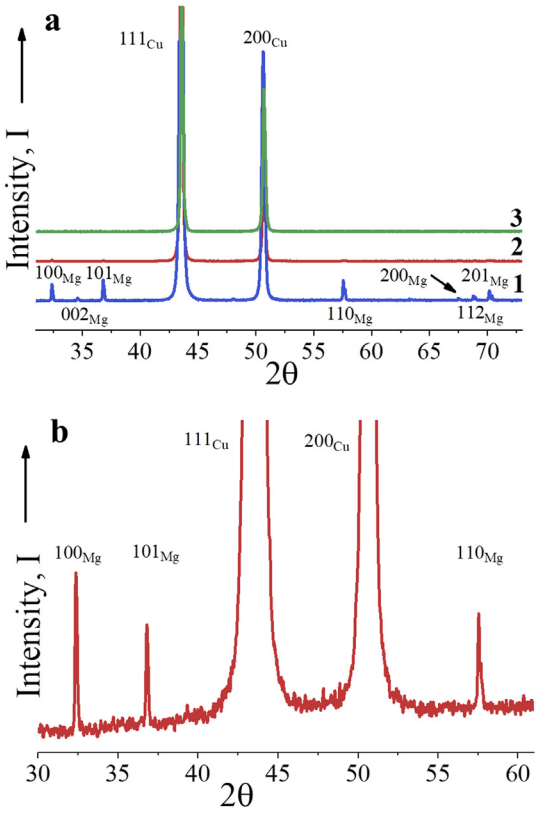

Fig. 9. XRD-results: (a) the spectra of the as-extruded Cu/Mg-composites with 1, 7 and 2730 Mg-filaments (diffractograms 1–3, respectively); (b) the visualization of the poor Mg-peaks at the X-ray spectra of the Cu/7 Mg-composite (it is a zoom of diffractogram 2 in (a) within the range of 2θ from 30° to 62°).

the same samples, which were demonstrated in Figss. 4–6. The X-ray spectrum of the Cu/1 Mg-composite contains both Cu-peaks and Mg-peaks (spectrum 1 in Fig. 9a). In turn, only Cu-peaks are clearly seen in the diffraction patterns of the composites with 7 and 2730 Mg-filaments in Fig. 9a. However, the XRD-result in Fig. 9b shows the presence of poor Mg-peaks against the background of very intensive Cu-peaks in the diffractogram of the Cu/7 Mg-composite. Despite the fact that a big number of very fine Mg-filaments are in the Cu/2730 Mg-composite (see Fig. 6b), XRD spectrum 3 in Fig. 9a does not show Mg-peaks in the corresponding diffraction pattern. It indicates that, in this case, the fraction of magnesium is below the detection threshold. Indeed, as shown in Table 1, the magnesium content in the Cu/2730 Mg-composite is very low.

In Fig. 9b, noteworthy is the absence of the $(002)_{Mg}$ peak. Moreover, at the diffractogram of the Cu/1 Mg-composite, the $(002)_{Mg}$ peak also has a very low intensity (see spectrum 1 in Fig. 9a). The absence of reflections from the basal planes indicates a strong texture in the Mg fibers. Obviously, in this case, all the "c" axes of the magnesium HCP lattice lie in the plane of the cross section of the composite rod. The formation of the sharp radial texture in the extruded rods of HCP-metals is well known [22].

As a whole, there is a very interesting feature in these XRD patterns. The Cu-peak changes its position towards to higher angles with increase in number of Mg-filaments and level of deformation strain. It is clearly seen in Fig. 10, where the X-ray diffraction pattern of pure Cu (spectrum 1) is superimposed on the XRD patterns obtained from the centers of the extruded Cu/2730 Mg-composite rods. For example, spectrum 2 in Fig. 10 was obtained from the composite rod of 6 mm in diameter with accumulated deformation strain $\eta = 13.7$. The peaks are even more displaced after additional deformation of this rod to Ø3 mm (spectrum 3 in Fig. 10). The

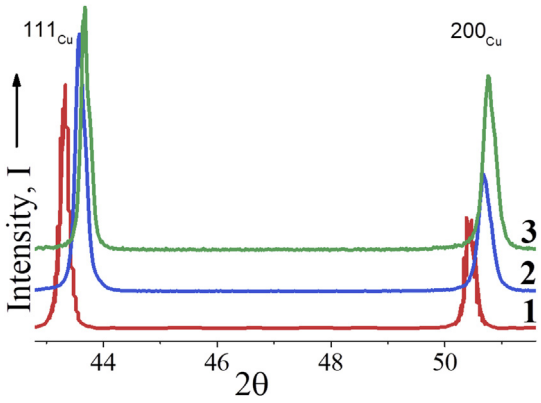

Fig. 10. XRD patterns of the copper (spectrum 1) and as-extruded Cu/2730 Mg-composite rods with different levels of deformation strain (spectra 2 and 3).

accumulated deformation strain of this rod is $\eta = 15.0$. Besides, SPD leads to broadening of XRD peaks due to the grain refinement and introduction of lattice strain. The same effects were discovered in Refs. [10,23] during the investigation of Cu–Nb microcomposite wires drawn to different strain values.

Based on the obtained XRD results, it was plotted a dependence of the lattice constant of Cu from the deformation strain of the Cu/Mg-composites under investigation (Fig. 11). It is well seen that the lattice constant of Cu is decreasing when the deformation strain is increasing.

3.7. TEM investigation

To observe the microstructure of the Cu/Mg-composites under investigation and confirm the solid solution formation at their interfaces, the TEM-method was applied. The wires of 0.25 mm in diameter of the Cu/7 Mg- and Cu/2730 Mg-composites were taken as samples for this observation. Such thin composite wires were used for the resistometric study in our investigation (see Figs. 7 and 8).

The TEM-image of the microstructure of the deformed Cu/7 Mg-composite is shown in Fig. 12. The accumulated deformation strain of this thin wire is $\eta \tilde{}12.5$. As it may be concluded from the plot in Fig. 11, such a high deformation level leads to a noticeable decrease in the lattice constant of Cu.

The long grains with widths from 100 to 700 nm are seen in Fig. 12a. As it may be concluded from the selected area diffraction pattern (SADP), all grains belong to the Cu-matrix only (Fig. 12b). A part of the grains has a high density of dislocations, which is

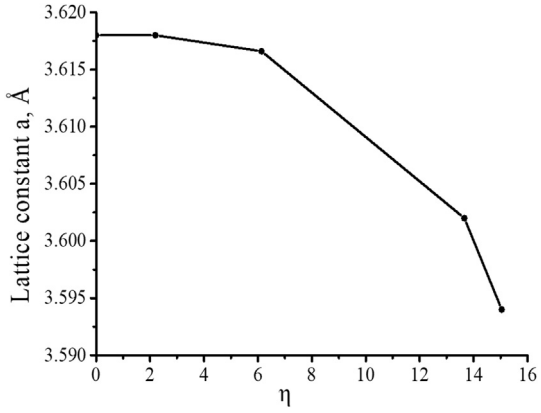

Fig. 11. Development of the lattice constant of Cu under deformation of the Cu/Mg-composites.

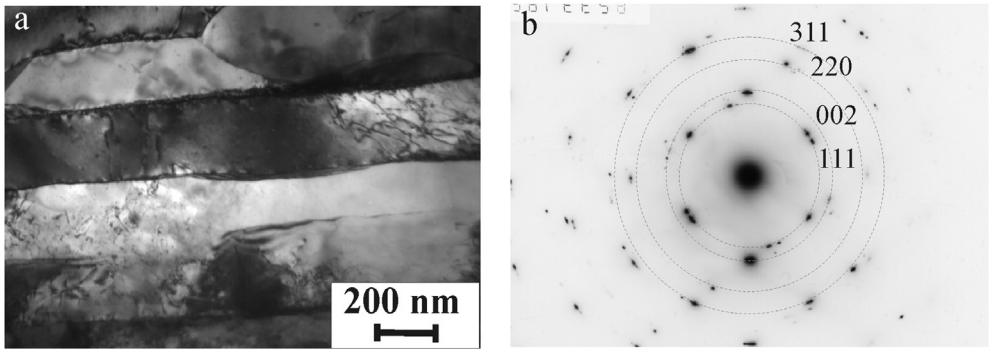

Fig. 12. Microstructure of the thin Cu/7 Mg-composite wire with accumulated deformation strain η~12.5: (a) bright field image of a typical microstructure; (b) selected area diffraction pattern of the microstructure (a): all rings correspond to fcc-Cu.

typical for the materials obtained by different SPD-methods [18,24,25]. The presence of extinction contours is clearly seen at the boundaries of these grains. It indicates that the grain boundaries and border areas are in a non-equilibrium state. The other part of the grains in Fig. 12a is almost dislocation-free. It may be concluded from this result that the processes of recrystallization are actively proceeding in the Cu-matrix during room-temperature SPD.

In the SADPs, which were obtained from the deformed Cu/7 Mg-composite, all the reflections were smeared azimuthally not more than 3° (Fig. 12b). We cannot find any phase other than copper in this sample (Fig. 12b). Moreover, the separation of the Cu-reflections or any additional reflections was not revealed. However, according to the measurements using the SADP in Fig. 12b, the lattice parameter of the Cu-matrix in the strong deformed Cu/7 Mg-composite is: a = 3.528 Å. Note that at the beginning of the study we measured the lattice parameter of the copper, which was used for making matrix in our experiment. The obtained value is a_{Cu} = 3.6179 Å (see the left point in Fig. 11). It may be concluded that the lattice parameter of the Cu-matrix decreases noticeably under SPD when making the thin Cu/7 Mg-composite wire. This result is a good match with the XRD-data in Fig. 11.

The microstructure of the deformed Cu/2730 Mg-composite is shown in Fig. 13. A significant contrast is seen within the long grains of the Cu-matrix (Fig. 13a,d). This contrast is caused by strong lattice distortions and a big number of dislocations both inside the grains and at the grain boundaries. The recrystallized grains are also observed in the microstructure of this composite.

We did not observe the Mg-filaments inside these two composites. This is mainly due to the rapid dissolution of magnesium in the electrolyte when preparing the Cu/Mg-samples for TEM-investigations. Therefore, only in some cases we were able to observe traces of magnesium and inclusions of the $CuMg_2$ intermetallic phase (Fig. 13b,d).

4. Discussion

The obtained results are of a significant scientific and practical interest. For example, the deformed Cu/2730 Mg-composite with minimal magnesium content has not only a low electrical resistance but also demonstrates a high strength. Moreover, the comparison of the plots in Figs. 7 and 8 allows concluding that the mechanisms of structure formation during the heating of the Cu/7 Mg-composite and Cu/2730 Mg-composite are significantly different. To clarify the features of the property formation of these composites, the structural transformations on their interfaces have to be studied in details. We have already started the structural investigations of the Cu/Mg-composites [26,27]. However, it seems that the results described above in combination with literature data are quite sufficient to understand the processes that occur in the composites under investigation.

Indeed, the discovered change in the lattice constant of Cu under the deformation of the composites may be related to dissolution of the Mg-filaments in the Cu-matrix. This feature is typical for the severe deformed composites. For example, the Nb dissolution in Cu (and vice versa) and related changes in the lattice constants of Cu and Nb were found during the deformation of the Cu/Nb-microcomposites [14]. Based on our results, we can conclude that the formation of SPD-induced Cu-based solid solution takes place on the Cu/Mg-interfaces in the process of making the composites. From this viewpoint, it would be also interesting to investigate the change in the lattice constant of Mg under deformation of the Cu/Mg-composites. However, it is not possible due to the fast disappearance of the Mg-peaks in XRD-patterns caused by the low content of magnesium in our composites (see Fig. 9).

As it is known from Ref. [6], in the Cu/Mg couple the diffusion of Cu-atoms is faster than that of Mg. In addition, it was revealed in Ref. [20] that $CuMg_2$ in Cu/Mg super-laminates composites can grow with a sufficient growth rate at low temperatures (less than 200 °C). These conclusions were made based on the results of experiments with heating the deformed Cu/Mg diffusion couple. We also observe the formation of the $CuMg_2$ intermetallic phase at the interface of the Cu/Mg-composites (Fig. 13). However, the thin wire of Cu/2730 Mg-composite that we investigated was obtained by SPD at room temperature. There are no reports in the literature on the accelerated diffusion of magnesium into copper (and vice versa) and formation of the $CuMg_2$ intermetallic phase in the Cu/Mg-couple as a result of the room-temperature SPD.

We believe that the formation of the Cu-based solid solution is actually the result of strain-induced effects rather than traditional diffusion mechanisms at the Cu/Mg-interfaces. Indeed, as we have already described above, it was observed that the copper sleeve was flowing faster that the magnesium core during the cold hydroextrusion of the composites. This phenomenon can be explained by the difference in the deformation mechanisms of Cu with its face-centered cubic crystalline structure and Mg, which has the hexagonal close packed lattice. This observation allows the conclusion that strong shear strains arise in the process of making Cu/Mg-composites. These deformation strains are very high and can be comparable with the ones that are realized using such a known SPD-method as high-pressure torsion (HPT) [9,28]. For example, the accumulated deformation strain of the Cu/2730 Mg-composite wire of 0.25 mm in diameter used for the resistometric study (Fig. 8) is $\eta \approx 20.0$. Such severe deformation and shear strains can lead to the synthesis of non-equilibrium phases [9,28,29].

Defining the composition of the new phases and clarifying the ratio of these phases in different sections of the mixed layer on the

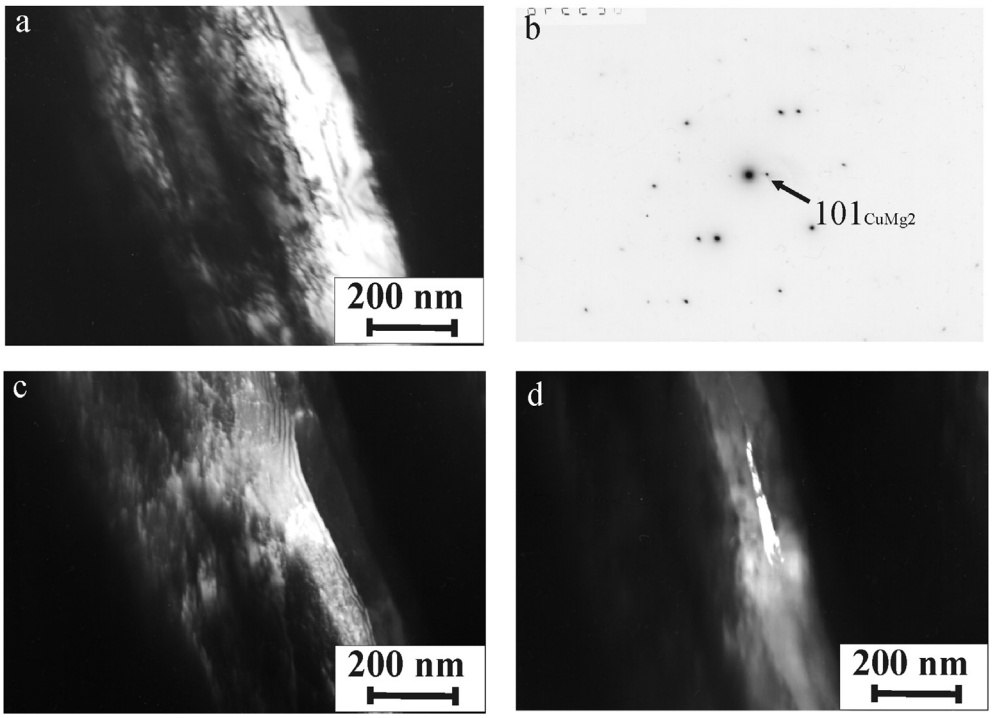

Fig. 13. Microstructure of the thin Cu/2730 Mg-composite wire with accumulated deformation strain $\eta \approx 20.0$: (a) bright field image; (b) SADP of the microstructure (a), the arrow indicates the reflection <101> of the $CuMg_2$ intermetallic phase; (c) dark-field image with g = <111> of copper: (d) dark-field image with g = <101> of the $CuMg_2$ intermetallic phase.

Cu/Mg-interface require performing a special structural study. However, using our results of the resistivity measurements, it is possible to do some assumptions. For example, copper-based solid solutions with different contents of solute elements were many times investigated before by resistometric methods [3,11,30]. It is established that the temperature dependence of the electrical resistivity of such alloys has a linear form [11,30]. The low temperature part of curve 1 in Fig. 8 also has a linear form. Nevertheless, a wide peak in the $d\rho/dT$ dependence near ~530°C indicates some transformation within this temperature interval. This temperature coincides with the temperature of formation of the fcc-Cu(Mg) solid solution from the two-phase structure (fcc-Cu(Mg) + Cu_2Mg) of the alloy which has just the same composition as the Cu/7 Mg-composite (see Fig. 1 and Table 1). Indeed, to obtain the Cu/2730 Mg-composite we inserted 390 thin wires of the Cu/7 Mg-composite in the Cu container. Obviously, almost all magnesium filaments should have been dissolved in the copper matrix to form the solid solution of the composition near 95.3Cu-4.7 Mg (at.%).

In our opinion, the following structural processes take place in the thin wire of the Cu/2730 Mg-composite. A supersaturated Cu-based solid solution is formed in the core of this composite wire after SPD with accumulated deformation strain $\eta \approx 20$. During the resistometric study, the decomposition of the supersaturated solid solution with precipitation of the Cu_2Mg phase takes place at the first stage of heating. With further heating, a single-phase fcc-Cu(Mg) solid solution is formed in this composite from two-phase structure (fcc-Cu(Mg) + Cu_2Mg) in the temperature interval from ~450 to ~600°C. As the peak in the $d\rho/dT$ dependence is wide (curve 3 in Fig. 8), it is obvious that different Cu-based compositions are formed in the core of this composite instead of a big number of thin Cu/7 Mg-composite wires. Within the high-temperature interval, the Mg-content in the core is fast decreasing due to Mg dissolution in the thick-wall of the Cu-sleeve because of the diffusion processes. As a result, the temperature dependence of the electrical resistivity in the process of cooling (curve 2 in Fig. 8) has a linear form that is typical for single-phase alloys [30].

The assumptions put forward here are completely consistent with the obtained experimental results. Indeed, the XRD-patterns (Fig. 10) and the change in the lattice constant during the plastic deformation (Fig. 11) point to the formation of a Cu-based solid solution in the core of the deformed Cu/2730 Mg-composite. The position of the wide peak in the $d\rho/dT$ dependence (curve 3 in Fig. 8) allows approximate composition determining of this solid solution. Based on these results, the conclusion may be that 2730 fibers of the supersaturated Cu-based solid solution were formed in the deformed Cu/2730 Mg-composite instead of 2730 Mg-filaments. As it was shown in Ref. [2], supersaturation with Mg provides excellent performances for solid-solution copper alloys, which is represented by an enhancement of strength. Therefore, the formation of the supersaturated Cu-based solid solution in the core of the deformed Cu/2730 Mg-composite allows explaining its high mechanical properties.

It should be emphasized here that the above description of the structure of highly deformed Cu/2730 Mg-composite is somewhat simplified. We did not consider here the effect of a small amount of pure magnesium, which we occasionally observed during the TEM-investigations. Neither did we take into account the presence of the $CuMg_2$ intermetallic phase at the composite interfaces (Fig. 13). Of course, both pure magnesium and the $CuMg_2$ intermetallic phase will contribute to the evolution of the microstructure and properties during heating of the Cu/2730 Mg-composite. However, as follows from the results of the resistometric study in Fig. 8, this contribution is small.

The question remains of why the Cu/2730 Mg-composite has a very low electrical resistance. Indeed, it is known from Refs. [2–4] that solid-solution Cu–Mg alloys exhibit poor electrical conductivity. Any solutes dissolved in copper act as electron scattering centers, and when their number increases, the electron mean free path decreases [3]. For example, a strong decrease in the electrical

conductivity of copper at the addition of 4.1 at.%Mg was shown in work [2]. As we believe, the Mg-content in the core of the Cu/2730 Mg-composite is very close to that in the Cu-4.1 at.%Mg alloy which was investigated in Ref. [2]. Nevertheless, the electrical resistivity of the Cu/2730 Mg-composite is just a little different from the electrical resistivity of copper (Table 4). The main reason of such differences is the design of the composite.

It is well seen in Fig. 6a that the Cu/2730 Mg-composite has a thick sleeve of pure copper. This Cu-sleeve will actually determine the electrical resistivity of the whole composite. It follows from the formula for calculating the electrical resistivity of the parallel conductors (4), where the conductor with the lowest resistivity makes the major contribution. These considerations are confirmed by the results of our resistometric study. Indeed, the electrical resistivity of the Cu/2730 Mg-composite increases a little after the experiment with heating of the sample to 750° followed by cooling (Fig. 8).

As it follows from Table 1, the composition of the Cu/2730 Mg-composite is: 98.9 at.%Cu - 1.1 at.%Mg. The electrical resistivity of the solid-solution Cu–Mg alloy with magnesium content of about 1,1 at.% is $\rho \tilde{} 2.2 \times 10^{-8}$ Ωm [3], which is very close to the electrical resistivity of the Cu/2730 Mg-composite sample after heating and cooling in Fig. 8. It may be concluded that a fast dissolution of magnesium in the Cu-sleeve at high temperature results to the transformation of the Cu/2730 Mg-composite into the single-phase Cu-based solid solution. However, the electrical resistivity of the deformed Cu/2730 Mg-composite in the beginning of this experiment is lower than that of solid-solution Cu–Mg alloy of the same composition resulted after heating and cooling.

One issue remained unresolved during this study. For example, we observed the gradual disappearance of Mg-peaks under SPD of the Cu/7 Mg-composites (Fig. 9). During the TEM-investigations, we only occasionally met traces of magnesium (Fig. 13). The temperature dependence of the electrical resistivity during heating of the Cu/2730 Mg-composite has a linear form up to ~450 °C (Fig. 8) that is typical for single-phase alloys [28]. All these results fit well the model, which we suggest, of Mg-filaments dissolution in the Cu-matrix under SPD of the Cu/Mg-composites. However, it is known, that the lattice parameter of Cu somehow increases at alloying with magnesium [31]. This contradicts our data. In our case, the dissolution of magnesium in the Cu-matrix leads to a decrease in lattice parameter of copper (Figs. 11 and 12).

Of course, the authors of work [31] studied the structure of Cu–Mg solid solutions in the equilibrium state. In turn, the structural state of the Cu-based solid solution formed in our highly deformed Cu/Mg-composites is extremely non-equilibrium. The formation of a number of metastable Cu–Mg phases was also noted in Ref. [31]. It can be assumed that the evolution of the microstructure at the interface of the Cu/Mg-composites under SPD is rather complicated and, possibly, proceeds with the formation of non-equilibrium and/or metastable phases. To understand the nature of the detected phenomenon, a separate large study of samples of the Cu/Mg-composites annealed at different temperatures is required. However, in the presented work, we considered only deformed composited rods and wires.

Thus, the hypothesis about the formation of the non-equilibrium Cu-based solid solution explains rather well the combination of the abnormally high strength and low electrical resistivity obtained in the severely deformed Cu/Mg-composites. In the near future, we plan to complete the corresponding microstructural studies. In conclusion, note that, in terms of combination of the mechanical and electrical properties, the deformed Cu/2730 Mg-composite is rather competitive in relation to the Conform-produced Cu–Mg-alloys with ultrafine-grained structures [4].

5. Conclusions

The study led to a number of interesting results. For example, our comparisons of the experimental strength with its theoretical estimation showed that the accuracy of the calculation is minimal if the volume fractions of the constituents are close. However, the accuracy of the theoretical estimate increases with an increase in the volume of any constituent of the composite. At the same time, it was confirmed that all model approaches have many limitations and, therefore, the results of such calculations should be treated with caution. The pronounced discrepancy remarked between the experimental and calculated yield strengths of the Cu/1 Mg-composite may be caused by the fact that the strain hardening behavior of Mg (with the hexagonal close-packed crystal lattice) is quite different from that of Cu (with the face centered crystal lattice). Moreover, the mechanical tests of the deformed composites revealed that the efficiency of the theoretical estimation of the strength is highly dependent on the volume of new phases formed at the Cu/Mg-interfaces. In turn, the known formula for the parallel conductors, which we used, allowed us to estimate the electrical resistivity of the Cu/Mg-composites with an acceptable accuracy.

The paper shows that SPD by hydroextrision followed by drawing leads to high mechanical properties of the Cu/Mg-composite, which contains 2730 Mg-filaments. The electrical resistivity of such an SPD material is only slightly higher than the electrical resistivity of copper. To explain the observed phenomena, we put forward an assumption about the formation of a supersaturated Cu-based solid solution at the Cu/Mg-interfaces during SPD of the composites. It is caused by severe deformation and shear strains, which arise in the process of making our composites and can lead to the formation of mixed Cu–Mg layers at the interfaces far beyond the equilibrium solution. This high-strength supersaturated solid solution inside the composite increases its strength and the thick Cu-sleeve provides low electrical resistivity. If this hypothesis is true, then a significant increase in the number and/or volume fraction of thin Mg-filaments will make it possible to obtain a high-strength Cu/Mg-composite with low electrical resistivity. We have already begun working in this direction and obtained a Cu/Mg-composite, which contains about one million fine magnesium filaments.

The Cu/Mg-composites we have studied may be of interest not only as conductors of electric current. For example, the $CuMg_2$ intermetallic compound has promising hydrogen absorption/desorption properties. Obviously, the $CuMg_2$ intermetallic compound can be easily formed in our Cu/Mg-composites by heating to ~500 °C (Fig. 7). Moreover, this intermetallic compound will be located inside the copper shell, which facilitates its practical application.

The next possible application of our development is related to biomedical applications. As is known, Mg-based alloys are very attractive as biocompatible and biodegradable metallic materials. The practical use requires various products of Mg-based alloys, including extra-fine wires, which may be used as implants in bone repair procedures and as cardiovascular stents in angioplasty. The technology developed by us is quite suitable for these purposes. Indeed, long and extra-fine Mg-wires can be obtained from Cu/Mg-composites by removing the Cu-matrix (for example, by chemical etching).

Thus, the results of the study are of interest in terms of developing new technologies in different areas.

Acknowledgments

The work was carried out in the framework of a state task according to the theme “Pressure” No. AAAA-A18-118020190104-3. The studies of structure and mechanical properties of the samples

were carried out at the Electron Microscopy Department and Mechanical Test Department of the Collective-Use Center of the Institute of Metal Physics (Ural Branch, Russian Academy of Sciences). The X-ray diffraction studies were carried out in the "Composition of Compounds" Center of Collaborative Access, Institute of High-Temperature Electrochemistry, Ural Branch, Russian Academy of Sciences.

Appendix A. Estimation of the deformation strain

To estimate the accumulated deformation strain (η) in the composites, we used the following equation:

$$\eta = e_{\,Cu/1Mg-composite} + e_{\,Cu/7Mg-composite} + e_{\,Cu/2730Mg-composite}, \quad (A1)$$

where (e) is the true strain of any composite under investigation.

$$e = 2\ln(d_o/d_f), \quad (A2)$$

where d_o and d_f are the initial and final diameters of the composite wire, respectively. In this case, the deformation strain of the Cu/7 Mg-composite can be found by equation:

$$\eta_{Cu/7Mg-composite} = 3.6 + 2\ln(d_o/d_f), \quad (A3)$$

where 3.6 is the true strain of the Cu/1 Mg-composite accumulated during the deformation from diameter 18 mm to diameter 3 mm (it is designated as $e_{Cu/1Mg\text{-}composite}$ in formula (A2)). Respectively, the deformation strain of the Cu/2730 Mg-composite is found by equation:

$$\eta = 3.6 + 7.5 + 2\ln(d_o/d_f), \quad (A4)$$

where 7.5 is the true strain of the Cu/7 Mg-composite accumulated during the deformation from diameter 21.5 mm to diameter 0.5 mm (it is designated as $e_{\,Cu/7Mg\text{-}composite}$ in formula (A1)).

Data availability

The raw/processed data required to reproduce these findings cannot be shared at this time as the data also make part of an ongoing study.

Author contribution

Alexey Yu. Volkov: Conceptualization, Methodology, Supervision, Discussion, Validation, Writing – original draft, review and edition. Boris D. Antonov: Investigation (X-ray analysis), Discussion. Evgenii I. Patrakov: Investigation (SEM), Discussion. Elena G. Volkova: Investigation (TEM), Discussion. Darya A. Komkova: Investigation (SEM), Discussion, Visualization, Writing – review and edition. Azambek A. Kalonov: Sample preparation (Hydroextrusion and Drawing), Investigation (Electrical resistivity measurements, Theoretical estimation) Andrey V. Glukhov: Sample preparation (Thermal treatment and Drawing), Visualization, Investigation (Mechanical tests).

References

[1] Zixin Huang, Zhong Zheng, Shan Zhao, Shijie Dong, Ping Luo, Lie Chen, Copper matrix composites reinforced by aligned carbon nanotubes: mechanical and tribological properties//Materials, & Design 133 (2017) 570–578, https://doi.org/10.1016/j.matdes.2016.08.021.
[2] S. Gorsee, B. Ouvrard, M. Goune, A. Poulon-Quintin, Microstructural design of new conductivity – high strength Cu-based alloy//, J. Alloy. Comp. 633 (2015) 42–47, https://doi.org/10.1016/j.jallcom.2015.01.234.
[3] Kazunari Maki, Yuki Ito, Hirotaka Matsunaga, Hiroyuki Mori, Solid-solution copper alloys with high strength and high electrical conductivity//, Scr. Mater. 68 (2013) 777–780, https://doi.org/10.1016/j.scriptamat.2012.12.0217.
[4] Chengcheng Zhu, Aibin Ma, Jinghua Jiang, Xuebin Li, Dan Song, Donghui Yang, Yuan Yuan, Jianqing Chen, Effect of ECAP combined cold working on mechanical properties and electrical conductivity of Conform-produced Cu-Mg alloys//, J. Alloy. Comp. 582 (2014) 135–140, https://doi.org/10.1016/j.jallcom.2013.08.007.
[5] Koji Tanaka, Hiroyuki T. Takeshita, Kosuke Kurumatani, Hiroshi Miyamura, Shiomi Kikuchi, The effect of initial structures of Mg/Cu super-laminates on hydrogen absorption/desorption properties//, J. Alloy. Comp. 580 (2013) S222–S225, https://doi.org/10.1016/j.jallcom.2013.03.155.
[6] Katsuhiko Nonaka, Toshiyuki Sakazawa, Hideo Nakajima, Reaction diffusion in Mg-Cu system//materials transactions, JIM 12 (1995) 1463–1466.
[7] Shaoyuan Lyu, Yanbo Sun, Guodong Li, Wenlong Xiao, Chaoli Ma, Effect of layer sequence on the mechanical properties of Ti/TiAl laminates//Materials, & Design 143 (2018) 160–168, https://doi.org/10.1016/j.matdes.2018.02.003.
[8] Huihui Nie, Wei Liang, Hongsheng Chen, Liuwei Zheng, Chengzhong Chi, Xianrong Li, Effect of annealing on the microstructures and mechanical properties of Al/Mg/Al laminates//Materials, Sci Eng A 732 (2018) 6–13, https://doi.org/10.1016/j.msea.2018.06.065.
[9] C. Suryanarayana, Mechanical alloying and milling//, Prog. Mater. Sci. 46 (2001) 1–184.
[10] Liping Deng, Zhifeng Liu, Bingshu Wang, Ke Han, Hongliang Xiang, Effects of interface area density and solid solution on the microhardness of Cu-Nb microcomposite wires, Mater. Char. 150 (2019) 62–66, https://doi.org/10.1016/j.matchar.2019.02.002.
[11] A.Yu Volkov, O.S. Novikova, A.E. Kostina, B.D. Antonov, Effect of alloying with palladium on the electrical and mechanical properties of copper//, Phys. Met. Metallogr. 117 (9) (2016) 945–954, https://doi.org/10.1134/S0031918X16070176.
[12] A.Yu Volkov, I.V. Kliukin, Improving the mechanical properties of pure magnesium through cold hydrostatic extrusion and low-temperature annealing// Materials, Sci Eng A 627 (2015) 56–60, https://doi.org/10.1016/j.msea.2014.12.104.
[13] B. Arcot, S.P. Murarka, L.A. Clevenger, Q.Z. Hong, W. Ziegler, J.M.E. Harper, Intermetallic formation in copper/magnesium thin films – kinetics, nucleation and growth, and effect of interfacial oxygen//, J. Appl. Phys. 76 (9) (1994) 5161–5170.
[14] Liping Deng, Ke Han, Karl T. Hartwig, Teo M. Siegrist, Lianyang Dong, Zeyuan Sun, Xiaofang Yang, Qing Liu, Hardness, electrical resistivity, and modeling of in sity Cu-Nb microcomposites//, J. Alloy. Comp. 602 (2014) 331–338, https://doi.org/10.1016/j.jallcom.2014.03.021.
[15] P.P. Wang, X.J. Wang, J.L. Du, F. Ren, Y. Zhang, X. Zhang, E.G. Fu, The temperature and size effect on electrical resistivity of Cu/V multilayer films, Acta Mater. 126 (2017) 294–301, https://doi.org/10.1016/j.actamat.2016.12.018.
[16] W.L.E. Wong, M. Gupta, Development of Mg/Cu nanocomposites using microwave assisted rapid sintering//Composites, Sci. Technol. 67 (2007) 1541–1552, https://doi.org/10.1016/j.compscitech.2006.07.015.
[17] Bo Feng, Yunchang Xin, Zheng Sun, Huihui Yu, Juan Wang, Qing Liu, On the rule of mixtures for bimetal composites//Materials, Sci Eng A 704 (2017) 173–180, https://doi.org/10.1016/j.msea.2017.08.0605.
[18] Liping Deng, Ke Han, Bingshu Wang, Xiaofang Yang, Thermal stability of Cu-Nb microcomposite wires, Acta Mater. 101 (2015) 181–188, https://doi.org/10.1016/j.actamat.2015.08.032.
[19] Kazuhiro Mitsui, Change in electrical resistivity during continuous heating of Cu_3Pd alloys quenched from various temperatures//, Philos. Mag. B 81 (4) (2001) 433–449.
[20] Koji Tanaka, Daiji Nishino, Kousei Hayashi, Shuki Ikeuchi, Ryota Kondo, T. Hiroyuki, Takeshita, Formation of Mg_2Cu at low temperature in Mg/Cu super-laminate composites during initial hydrogenation//, J. of Hydrogen Energy 42 (2017) 22502–22510, https://doi.org/10.1016/j.ijhydene.2017.02.193.
[21] M. Gupta, W.L.E. Wong, Magnesium-based nanocomposites: lightweight materials of the future, Mater. Char. 105 (2015) 30–46, https://doi.org/10.1016/j.matchar.2015.04.015.
[22] I.L. Dillamore, W.T. Roberts, Preferred orientations in wrought and annealed metals//, Metall. Rev. 10 (1965) 271–380, https://doi.org/10.1179/mtlr.1965.10.1.271.
[23] K.M. Youssef, M.A. Abaza, R.O. Scattergood, C.C. Koch, High strength, ductility, and electrical conductivity of in-situ consolidated nanocrystalline Cu-1%Nb// Mater, Sci. Eng. A 711 (2018) 350–355, https://doi.org/10.1016/j.msea.2017.11.060.
[24] O.V. Antonova, A.Yu Volkov, Change of microstructure and electrical resistivity of order Cu-40Pd (at.%) alloy under severe plastic deformation//, Intermetallics 21 (2012) 1–9, https://doi.org/10.1016/j.intermet.2011.09.004.
[25] Mohammad Reza Toroghinejad, Rooholah Jamaati, Dutkiewicz Jan, A. Jerzy, Szpunar. Investigation of nanostructured aluminum/copper composite produced by accumulative roll bondind and folding process, Mater. Des. 51 (2013) 274–279, https://doi.org/10.1016/j.matdes.2013.04.002.
[26] A.Yu Volkov, A.A. Kalonov, D.A. Komkova, A.V. Glukhov, Structure and properties of Cu/Mg-composites produced by hydrostatic extrusion//, Phys. Met. Metallogr. 119 (10) (2018) 946–955, https://doi.org/10.1134/S0031918X18100125.
[27] I.G. Brodova, A.Yu Volkov, I.G. Shirinkina, A.A. Kalonov, T.I. Yablonskikh, V.V. Astaf'ev, L.V. Elokhina, Evolution of the structure and properties of Al/Cu/Mg ternary composites during thermomechanical treatment//, Phys. Met. Metallogr. 119 (12) (2018) 1210–1216, https://doi.org/10.1134/S0031918X18120050.

[28] Yuanshen Qi, Kosinova Anna, Askar R. Kilmametov, Boris B. Straumal, Eugen Rabkin, Plastic flow and microstructural instabilities during high-pressure torsion of Cu/ZnO composites//Materials, Character 145 (2018) 389–401, https://doi.org/10.1016/j.matchar.2018.09.001.
[29] K. Wongpreedee, A.M. Russel, The stability of Pt nanofilaments in a Au-matrix composite//Gold, Bulletin 40 (3) (2007) 199–205.
[30] J. Freudenberger, A. Kauffmann, H. Klaub, T. Marr, K. Nevkov, V. Subramanya Sarma, L. Schultz, Studies on recrystallization of single-phase copper alloys by resistance measurements, Acta Mater. 58 (2010) 2324–2329, https://doi.org/10.1016/j.actamat.2009.12.0618.
[31] A.A. Nayeb-Hashemi, J.B. Clark, The Cu-Mg (Copper-Magnesium) system//, Bulletin of Alloy Phase Diagrams 5 (No.1) (1984) 36–43.